Civil Engineering Infrastructures Journal 2021, 54(1): 23-42
DOI: 10.22059/ceij.2020.287489.1607

RESEARCH PAPER

Investigating the Reliability of Negative Skin Friction on Composite Piles

Hajitaheriha, M.M.[1], Jafari, F.[2], Hassanlourad, M.[3]* and Hasani Motlagh, A.[4]

[1] PhD Student, Department of Civil Engineering, Memorial University of Newfoundland, NL, Canada.
[2] M.Sc., Department of Civil Engineering, Malayer University, Malayer, Iran.
[3] Associate Professor, Department of Civil Engineering, Imam Khomeini International University, Qazvin, Iran.
[4] PhD Student, Department of Civil Engineering, University of Calgary, Alberta, Canada.

Received: 18 Aug. 2019; Revised: 22 Nov. 2020; Accepted: 02 Dec. 2020

ABSTRACT: In this study, the impact of Negative Skin Friction (NSF) on composite piles concerning different variables such as different pile sections, the amount of concrete and steel consumption, and various interaction coefficients of the pile-soil system in both solid and hollow conditions are evaluated using numerical methods. Besides, the effect of the variables considered on the negative skin friction and pile's settlement is investigated. Numerical analyses were performed using ABAQUS and MATLAB. The results showed that the amount of frictional stress on the pile decreases if the hollow sections are used. However, the hallow pile experiences more settlements than other piles' models. On the other hand, if the amount of consumed steel in a pile is reduced, the amount of negative skin friction induced in a pile decreases, while the pile settlement increases. After examining the Finite Element of concrete piles in fine-grained soils, the safety surface of the suggested numerical relationship was considered in the phenomenon of negative friction on the pile. For this purpose, considering the uncertainty parameters such as mean, variance and probability function for overcharge, soil parameters, dimensions and different types of the single pile, the amount of settlement, the stress created on the pile, the position of neutral plane on the pile and drag load were calculated using the proposed relationship. Finally, the safety surface of the proposed relationships or comparisons of a Finite Element results in a close approximation to the real models was computed.

Keywords: Drag Load, Negative Skin Friction, Neutral Plane, Reliability, Uncertainty.

1. Background

Traditionally, in the foundation design of infrastructures, engineers have used fixed deterministic values for the load acting on the deep foundation as well as its load-bearing capacity. However, these values are not unique and have probability distributions which reflect many uncertainties on the strength of the deep foundation. Reliability evaluation provides an approach for a unified geotechnical and

* Corresponding author E-mail: Hassanlou@eng.ikiu.ac.ir

structural framework for risk assessment, propagation of uncertainties, and national boundaries. The Reliability-Based Design (RBD) equations are required for common; the aim of the RBD implementation is usually to achieve an appropriate factor of steady and more affordable design.

In the past three decades, different approaches were applied for mitigation of geo-hazards and establishing a higher performance of geotechnical works. For instance, using nonlinear effective stress analysis of soil-structure systems introduced on bearing capacity of pile foundation and experimental studies through geotechnical centrifuge tests are of these approaches.

The main factors for hazardous geotechnical phenomenon can be the decreased stability of structures induced by the transient inertial loads, laboratory errors, scarcity of data, lack of uniformity of soil properties and sometimes insufficient knowledge in problem detection. For example, pile foundations in the saturated sand deposits are more often used for structures built on reclaimed lands. The apparent cause of these failures is the excess settlement and lateral force due to the inertia force of huge-structures and soils which embed foundations during services. Therefore, it is essential to realize the failure mechanisms of such components in NSF phenomenon to improve their performance against drag load and down drag to conserve the long-term stability of the structure, and save money and people's life.

Due to the new investigation of NSF through effective stress analysis, this method of design is becoming more common in the mega infrastructures including high rise buildings, port communities, and marine transportation. The exposure time and allowable limit state (i.e. load, deformation, curvature, and moment) are general terms of specified criteria. Additionally, the permanent deformations represented by the function of ground motions of design-level are not addressed in the guidelines as a main concern in the performance-based design. The design of infrastructures considering NSF and drag load and settlement are categorized as complex technical problems and a large number of issues related to the design process require further research and refinements.

2. Literature Review

Failure of piled foundations is a worldwide designing concern. One of the main reasons goes back to the NSF phenomena, which is attributed to the effects of increased pile's settlements as a result of negative friction stress. Ditlevsen and Madsen (2007) studied that the NSF was mobilized in the ultimate limit, except for the vicinity of the neutral plane. Thus, drag load may lead to the structure collapse when the recommendations of pile design are ignored. A number of failure reports can be found pertaining to the drag load, down drag and NSF on single piles.

Xing and Liu (2018) studied the NSF influencing factors on pile foundations in collapsible soils. The primary factors analysed in their research were pile type, different loess collapsibility, and cumulative relative collapse amount. Eslami et al. (2020) studied the significance of scale influences and their role on making a direct relation between pile shaft capacity and CPT records. A database was prepared including 83 full-scale CPT records and pile load tests to validate and calibrate the proposed approach.

Hajitaheriha et al. (2015) investigated the negative skin friction on single batter and vertical piles. A skin friction and vertical end-bearing piles under different loadings were considered to evaluate the neutral plane location and the down-drag. The performances of the friction pile and end-bearing piles considering different inclination angles were evaluated. They revealed that the position of neutral plane and the drag load of the pile depend on the type of pile, inclination angle of pile,

surrounding soil of the pile, earth surface loading intensity, and model type.

Azizkandi et al. (2019) conducted an experimental study on a square foundation to assess the effect of S/D and L/D parameters on non-connected and connected eccentric raft system of pile. In the non-connected raft system of pile showed that increasing the pile length not only does not significantly increase the bearing capacity, but also had lower effects on the settlement reduction. Pastor et al. (2018) carried out a study on skin friction of cement pastes in micro-piles when grout surface is imposed to the sulphates. They studied the friction variations depending on the initial sample roughness and friction of cement paste.

Jinyuan et al. (2012) investigated various influencing factors on the NSF of a pile, including the soil-pile interface, consolidation time, coefficient of lateral earth pressure, surcharge intensity, limiting displacement of soil-pile, stiffness of the bearing layer, and soil compressibility. The results showed that the neutral plane is mainly dependant on the consolidation time and the stiffness is mainly dependant on the bearing layer. Cao et al. (2014) developed a load transfer hyperbolic model as for soil-pile interface based on soil-structure interface tests, which considered the development of shear strength at the soil-pile interface, the characteristics of increasing initial shear stiffness, the loading, unloading, and reversed shearing behaviour of the soil-pile interface with consolidation.

El-Mossallamy et al. (2013) used a Fnite Element and axisymmetric model to analyze, and simulate the soil-pile interaction of negative skin friction. The pile and soft soil were simulated by a linear elastic model and double hardening soil model, respectively. A case study for two instrumented end bearing driven precast concrete piles was back analyzed in Bangkok soft clay. Various approaches for load configuration and pile element modelling were considered. Haghbin et al. (2016) developed an analytical model in order to assess the seismic bearing capacity of a strip foundation located on a reinforced slope with rows of piles. The passive pile resistance was determined based on shear and normal stress of the pile's surrounding soil that compared to other analytical methods. This study determined and established the relation between seismic bearing capacities and various parameters of the footing to obtain the optimum locations of pile rows which present the best improvement in the foundation's seismic bearing capacity.

Huang et al. (2015) conducted experimental model tests on the negative skin friction of pile groups in sand. The layered settlement of soil, pile top displacement, and pile stress and were examined under various surcharge loads. The results indicated that a single pile's neutral plane varies from 0.8×L to 0.95 length of pile in sand as the surrounding load increases from 20 to 120 kPa. Although the neutral plane's location was higher, the negative skin friction and pile head settlement under surrounding load were bigger compared with the results of the test under side load.

Gang-qiang et al. (2014) developed a model to calculate the negative skin friction of special-shaped pile considering pile-soil interaction under surcharge. Considering the influence factors, including the diameter of the pile base, the taper angles, pile-soil interface parameters, and surcharge were analysed based on the theory of concentric cylinder shearing. This study revealed that the proposed approach could effectively analyse the negative skin friction of a special-shaped pile under surcharge.

Golafzani et al. (2019) assessed various predictive models in the RBD framework by considering SPT and CPT-based methods and various static analyses in order to evaluate resistance factors and reliability indices. Also, resistance factors of Load Resistance Factor Design (LRFD) were calibrated for various loading ratios and reliability indices. Fardis et al. (1982) set up

liquefaction probability models to investigate the variability of the soil liquefaction's major parameters by implementing the linear first-order and second- moment method.

Moshfeghi and Eslami (2018) investigated six cone penetration tests by assigning the bearing capacity of DDP. In order to evaluate the results of the reliability-based and statistical methods, performance assessment of the methods considering pile–soil characteristics was applied. Carswell et al. (2015) used probabilistic methods to evaluate the reliability of pile foundations under offshore wind turbine with respect to serviceability limit states in a two-dimensional non-linear pile–spring model considering the soil springs by implementing Euler-Bernoulli beam elements.

Juang et al. (2012) examined the reliability of soil liquefaction potential by using the first-order reliability method. They established an empirical equation through neural network learning based on cone penetration tests to determine liquefaction potential with respect to cycle resistance ratio. Jha et al. (2009) used a simplified approach to determine the probability of liquefaction with its factor of safety based on a FOSM method, an advanced FOSM reliability method, a Monte Carlo simulation method, and a point estimation. The minimum factor of safety value for soil liquefaction analysis according to the variability of shear stress parameters, acceptable risk and soil resistance had been studied and a new design factor of safety was proposed.

3. Modeling and Calibration

Profile of the modelled soil was implemented based on the Lee et al. (2002) research and the impacts of negative skin friction on both down drag and drag load were studied. Further, the reliability method for this model and different piles' types was analysed. The pile was considered elastic with 0.5m in diameter and 20m in height. The soil profile was layered, including a top soft clay layer laid over a bottom dense sand layer. Besides, the pile shaft was set in the soft clay and its end was placed on the dense sand. Soil layers were assumed to behave as an elastic-plastic material with the Mohr-Coulomb shear failure envelope. Soil and pile material properties are summarized in Table 1.

Meshes, stratification and geometry of the model made by the 3-D Finite Element ABAQUS software are shown in Figure 1.

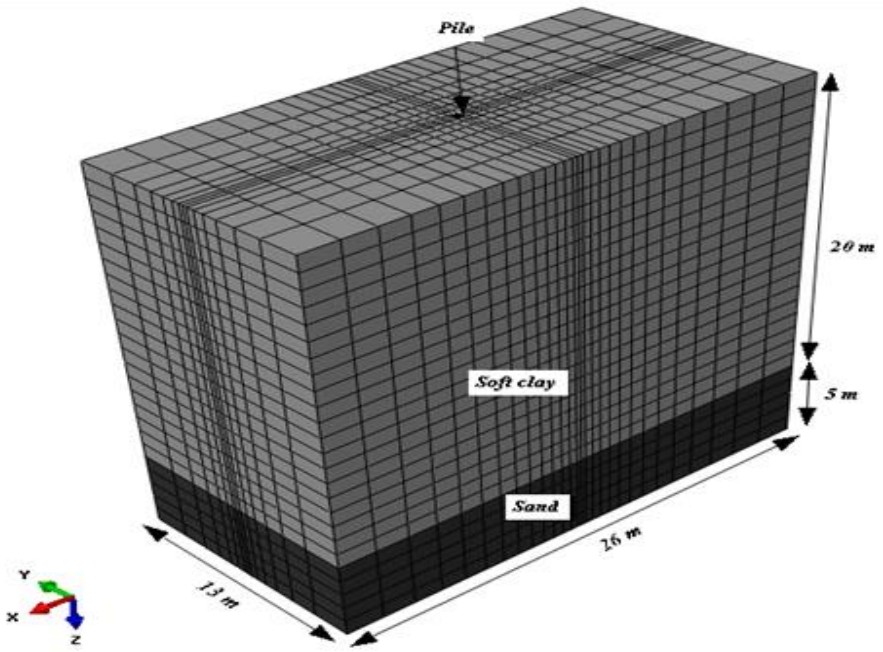

Fig. 1. The sections used in numerical modeling in ABAQUS software

Table 1. Material properties used in the analysis by Lee et al. (2002)

Material	Model	E (kPa)	C (kPa)	ν	ϕ (º)	Ψ (º)	K_o	γ (kN/m^3)
Concrete pile	Isotropic elastic	20,000,000	-	0.3	-	-	1.0	25
Soft clay	Mohr-Coulomb	5000	3	0.3	20	0.1	0.65	18
Dense sand	Mohr-Coulomb	50,000	0.1	0.3	45	10	0.5	20

The soil element's size in the proximity of the pile is considered finer in order to increase the accuracy of the analysis, however, the size increased by moving away from the pile vicinity to avoid a large computational cost. The model's boundaries are considered far enough from the pile to prevent stress conflict. First, the model was solved to obtain in-situ stresses. Before the main analysis, the initial displacements were set zero and the soil-pile interactions were ignored. The soil in the in-situ stresses and the soil hardening due to the pile installation were also overlooked.

The stiffness of both lower and upper soil layer was assumed to be identical in order to model the frictional pile for the NSF analysis. However, the stiffness of the lower soil layer was assumed to be 1000 times bigger than the upper soil layer for the end-bearing pile. Mohr-Coulomb shear failure criterion properly defines the constitutive model for the soil-pile interface elements. The interface elements are allowed to be separated when a gap is formed along with the soil-pile interface and tension is developed across the interface.

The normal and shear forces are set to zero. The interface friction coefficient (μ) was multiplied with the normal effective stress (σ') of the two contact surfaces to get a frictional shear stress as $\tau = \mu.\sigma'$. When the shear stresses applied along the interfaces become less than τ, the surfaces will stick together.

It has been found that the pile behaviour is mainly governed by the interface behaviour. Coefficients of in-situ pressure (K_0) were considered by the Jaky (1948) method for dense sand and normally consolidated clay as 0.65 and 0.5, respectively. The interface frictional coefficient ($\mu = tan(\delta)$) was supposed to be as 0.3-0.4. As shown in Figures 2 and 3, shear stresses obtained from the axial drag load and skin of the pile is very close to Lee et al. (2001). Simplified models assumed the mobilization of shear strength below and above the pile neutral line, however, the analysis by ABAQUS software provide a platform in order to consider the shear strength's partial mobilization according to the applied shear strain.

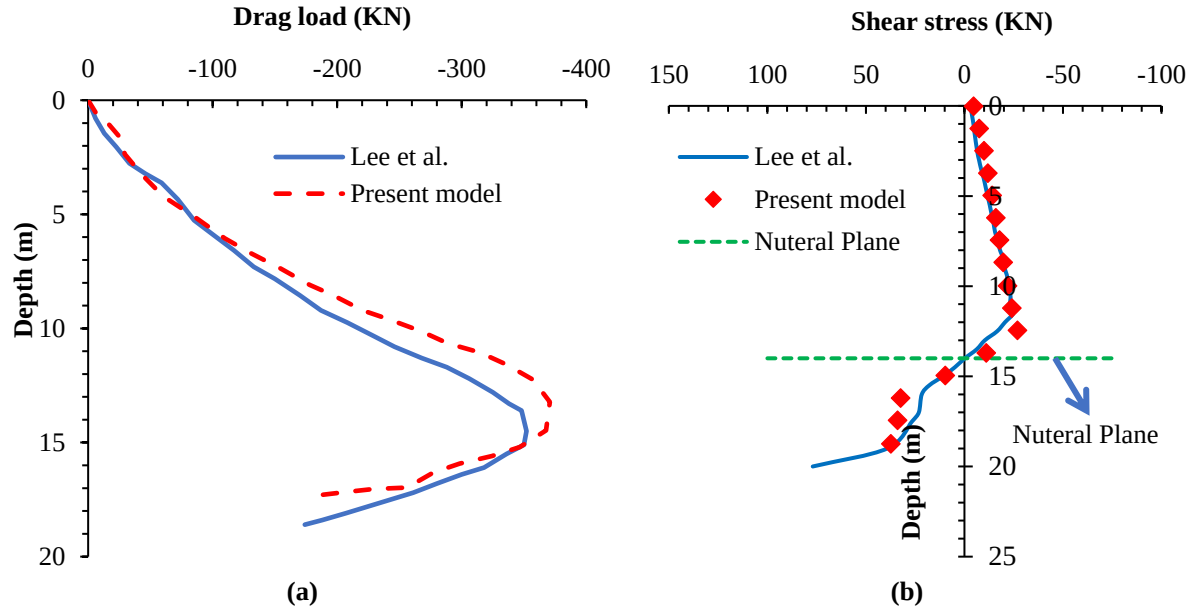

Fig. 2. a) Shear stress distributions along with the pile surface and; b) Axial drag load for a single frictional pile

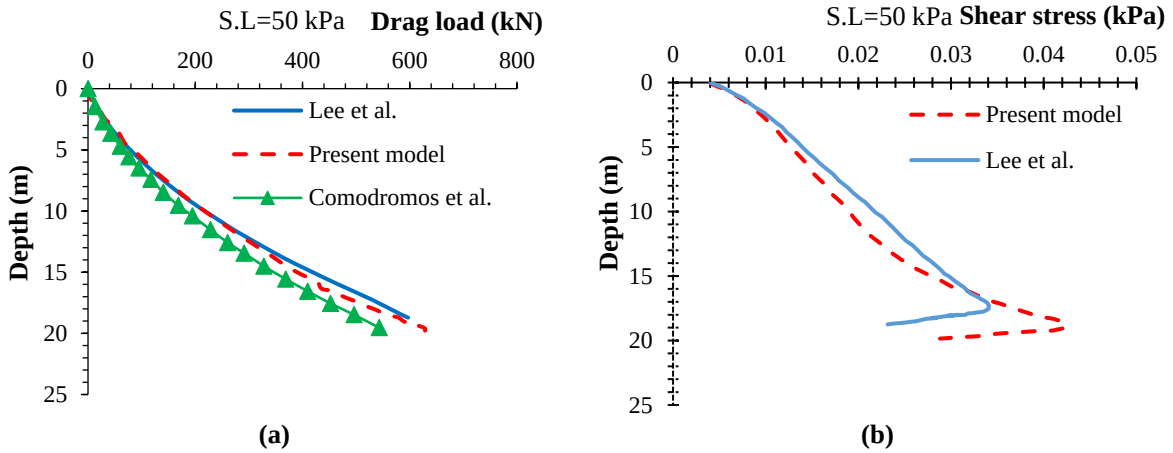

Fig. 3. a) Shear stress distributions along with the pile surface and; b) Axial drag load for a single end-bearing pile

4. Models

Figure 4 shows the models used in the study. Models a and b, are assigned to the model with circular and square cross-sectional while their shells are steel. The c and d models are related to the square and circular concrete hollow sections, and the model e and f are filled concrete piles. The elastic modulus, the soil's properties and the type of used concrete in all models are considered the same as each other so that the power of comparison between the created models can be possible and obvious. In order to compare the results with the Lee (2001) findings, it is tried to consider the dimensions of the model, soil and pile types the same as the laboratory model.

The results of the soil and pile's settlement are shown in Figures 5 to 12. Pile settlement results in Figures 5 and 6 show the finding for composite models a and b. Also, Figures 9 and 10 show the results of concrete piles. The results of these four figures show that the steel elastic modulus is about 10 times more than that of concrete. So, the rate of soil settlement has decreased around the concrete.

The settlement of concrete pile into the soil was found to be much larger than steel-concrete pile, and the settlement of the surrounding soil was even more with concrete pile due to its faster settling. The side of the square section is 0.5 m and is equal to the circular diameter. It is expected that the use of steel in the shell of the pile will reduce the pile settlement, because the density and modulus of steel are more significant than that of concrete pile. Also, the steel pile creates less interaction coefficient between the pile's shell and the soil.

According to Figures 5 and 6, which are related to the simple square and circular composite piles, respectively, the neutral plane depth in the square sections is greater than the circular sections. This reflects the fact that the longer length of the pile is exposed to the negative friction. Therefore, in addition to the further settlement in the surrounding soil and pile, the length of the pile, which is affected by the NSF, obtained more. It is also expected that with the reduction of the pile's mass by making the pile section hollow, the amount of pile settlement will increase.

Figures 7 and 8 show the results of the models c and d, which are related to hollow piles and soil put in the hollow section to the effects of overburden at the end of the pile were considered. The settlement of the square sections is higher than the circular sections in all models. On the other hand, the amount of settling in the hollow piles is higher than the total and composite piles. Figure 11 shows that if the differential settlement between the piles and the soil is greater, the neutral plane has put into the depth of the soil and the geometric fit between the neutral plane and this differential settlement has been governed.

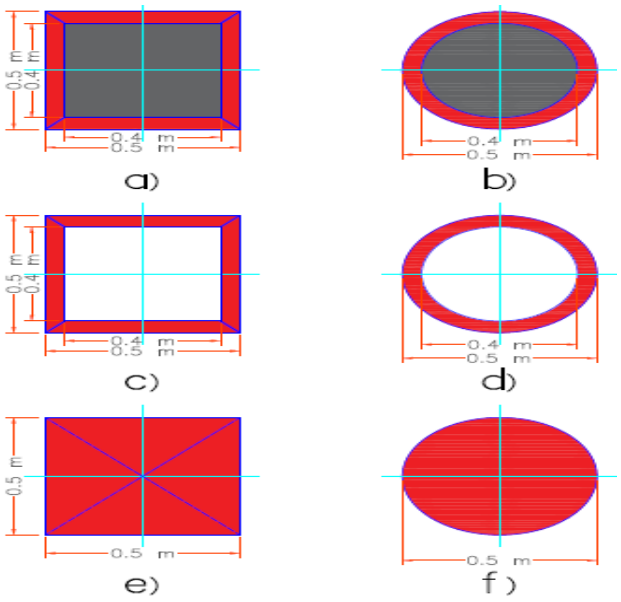

Fig. 4. The Finite-Element mesh of a single vertical pile and a soil profile: a) Square composite pile; b) Circular composite pile; c) Hollow square pile; d) Hollow circular pile; e) Concrete square pile and; f) Concrete circular pile

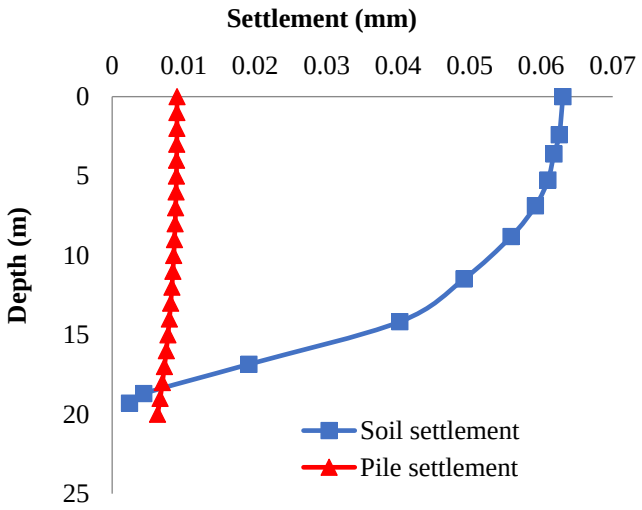

Fig. 5. Square composite model (model a)

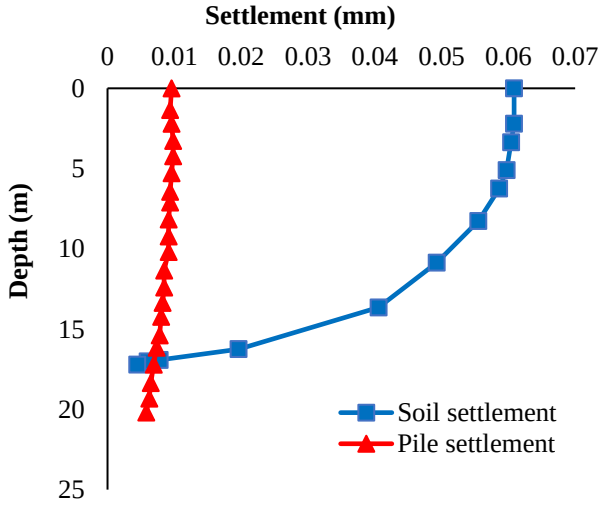

Fig. 6. Circular composite pile (model b)

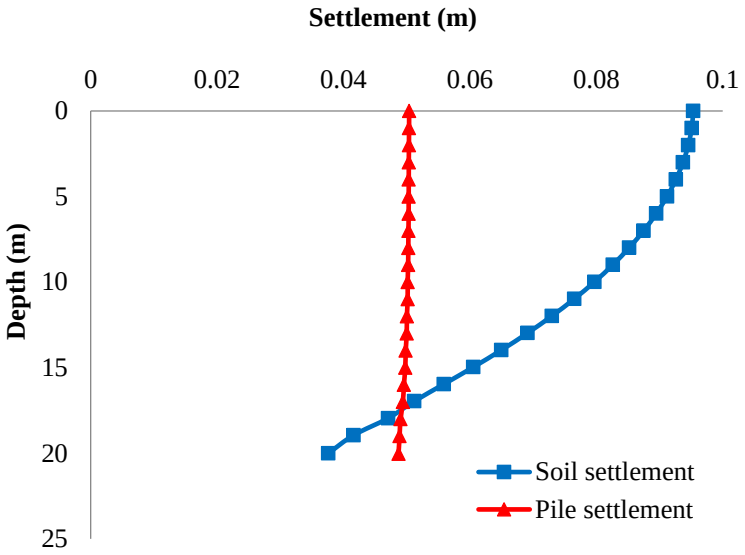

Fig. 7. Settlement of square pile for the concrete model (model c)

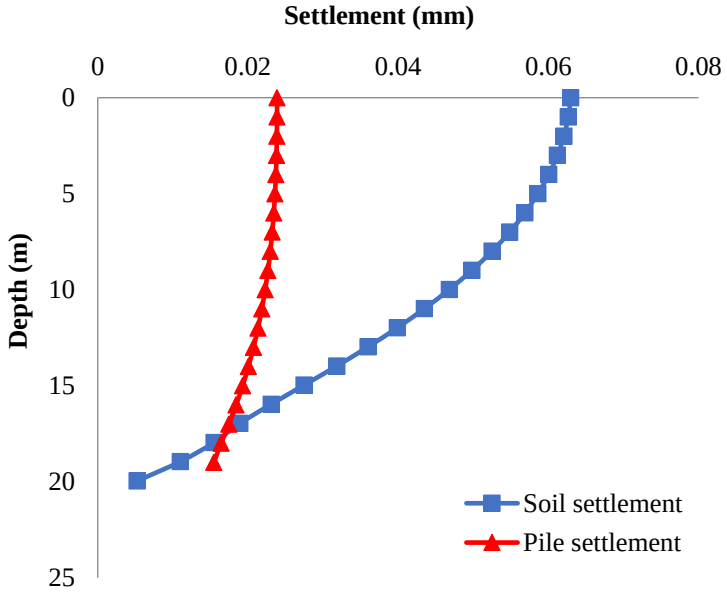

Fig. 8. Settlement of square pile for the concrete model (model d)

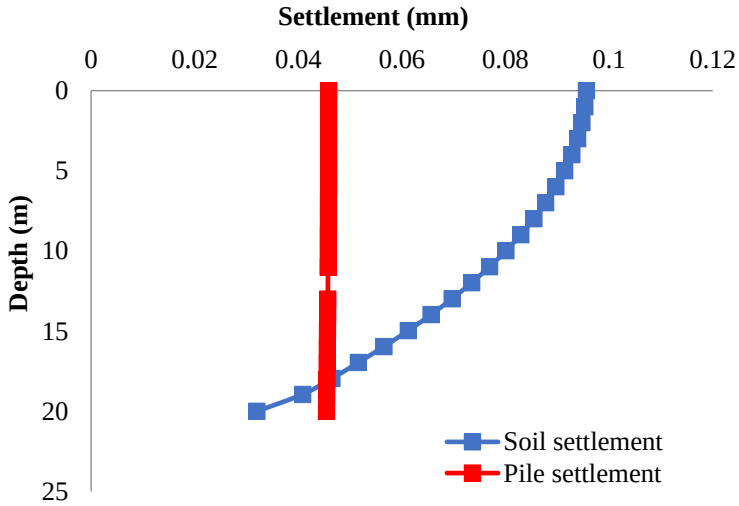

Fig. 9. Settlement of square pile for the concrete model (model e)

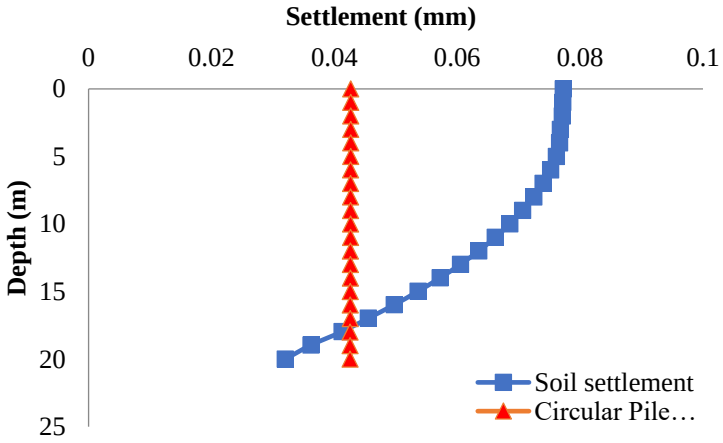

Fig. 10. Settlement of circular pile (model f)

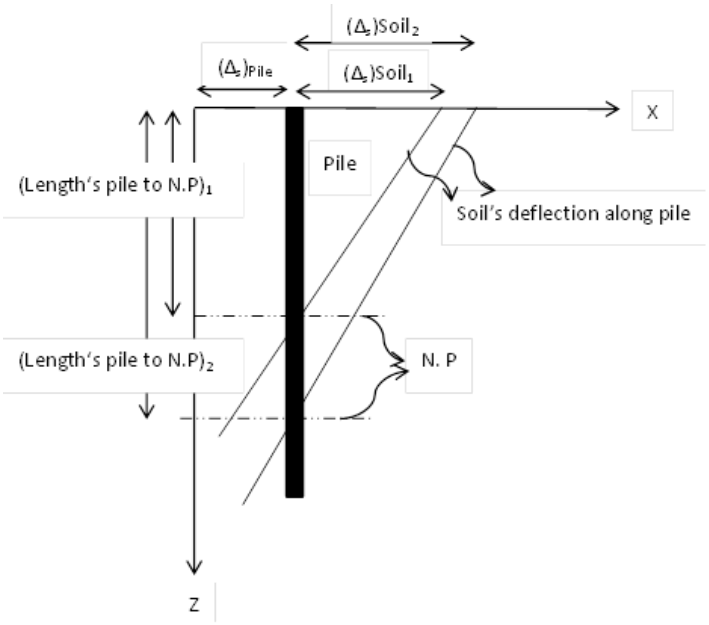

Fig. 11. The geometry of differential deflections of pile and soil to neutral planes

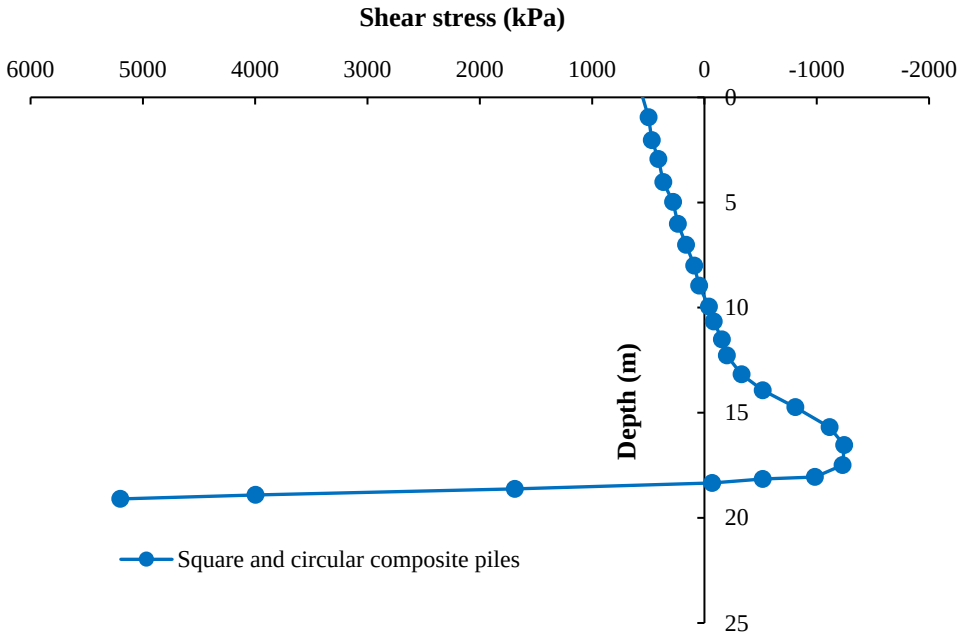

Fig. 12. Square and circular composite piles

5. Analysis of Results

The results of frictional stresses for different models are presented in this part. Figure 12 shows the amount of frictional stress for the composite square and circular sections. At this point, the value of negative frictional stress is lower in comparison with other sections. Figures 13 and 14 show the amount of the produced frictional stress in a pile for the square and circular sections in both fill and hollow types. It can be seen that the amount of the generated positive frictional shear stress in the hollow sections is less than the filled pile sections due to the reduction in mass. In the other words, the pile shell's resistance to the negative skin friction phenomenon has decreased and the pile and its surrounding soil experience more settlement.

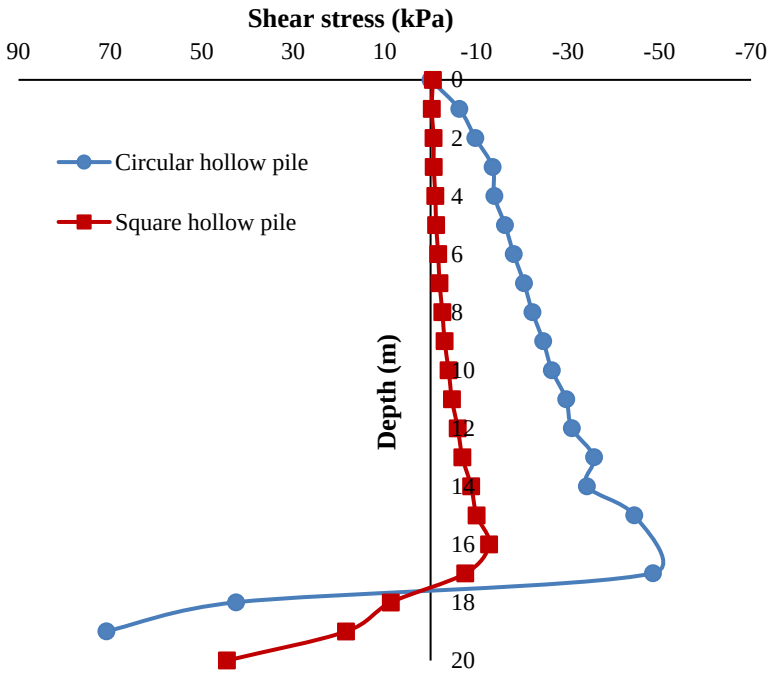

Fig. 13. Square and circular hollow piles (models c and d)

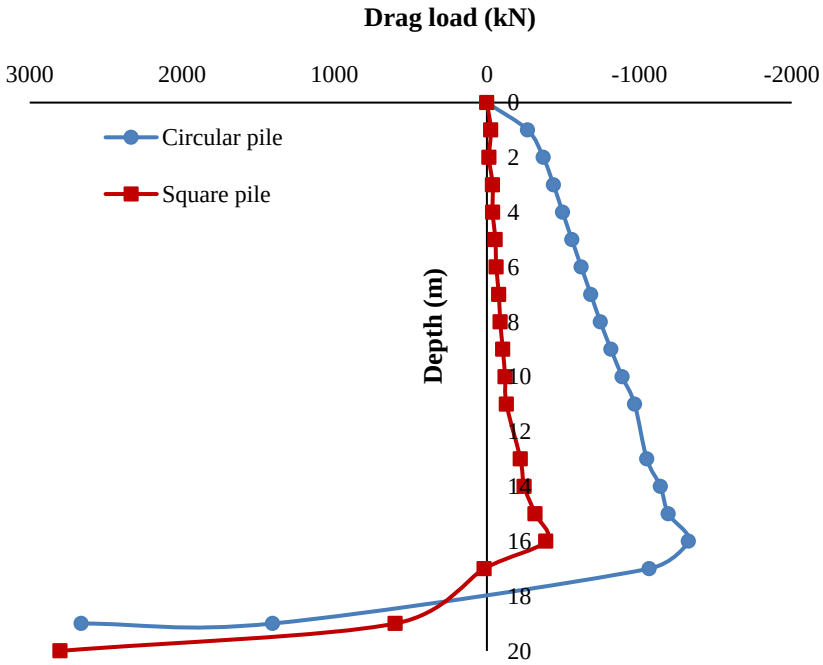

Fig. 14. Square and circular piles (models e and f)

On the other hand, in the circular hollow sections, the depth of the neutral plane has increased to some extent, which shows that the elements of the pile have been affected by the negative frictional stress. Positive frictional stress after neutral plane depth has decreased sharply in the hollow sections, which shows that the use of friction pods in fine-grained soils leads to an increase in the pile settlement and a resistance reduction under applied overheads.

It can be noted from Figures 13 and 14 in square and circular piles that by increasing the side area in the square sections, the amount of positive and negative shear stress is dropped in the soil. However, the reduction in negative friction stress was significantly higher than the negative frictional stress. Therefore, it can be concluded from the comparison of the numbers that the rate of the negative shear stress at the level of the circular piles was higher than that of the square sections. However, the reduction in frictional stress was significantly higher than negative friction.

Thus, by comparing the numbers, it is concluded that the rate of the negative shear stress at the level of the circular pile was higher than that of the square sections. The amount of positive frictional stress produced in the circular sections is approximately 1.5 times than of square sections. It can be said from the Figures 9 and 10 that in the pile's square sections, settling of these piles are more and positive; however, the negative frictional shear stresses are lower than the circular sections.

6. Investigation of Drag Load in Pile's Shell

In this part, the effect of piles' drag load on the mentioned composite piles is investigated. The amount of cumulative frictional force created by the overcharge is obtained from the product of the side area of the pile × frictional stress throughout the pile's shell.

Figure 15 illustrates the positive drag load value of square and circular sections. In the circular sections, the amount of negative frictional force results in the negative frictional stress which is far more than the square sections.

7. Hollow Sections

As is clear from Figure 16, the positive drag load value is 1778 kN in the square concrete sections, while this value is 2222 kN in circular ones. It can be said that more frictional force has been generated in square sections. The amount of negative drag load force created during the square pile is 525 kN, while this value is 1525 kN in the circular- section pile. In other words, in the circular section pile, the amount of negative frictional force that results in the negative frictional stress is far more than the squared section pile.

8. Discussion

In this study, the behaviour of individual piles in different dimensions and different materials concerning the effect of frictional negativity is evaluated. The piles under the load and the lateral surface are examined in the same way. In Tables 2 and 3 the shear stress in individual pile's shell is studied in different states.

In the square sections of the steel shell, the shear stress is in the highest amounts (in the neutral plane) than the other models. As the steel-soil interaction is less than of concrete-soil, the force mobilization of the pile's shell becomes less than the other models. Therefore, the lower shear stresses in composite piles with a steel shell are observed. On the opposite side, on the hollow pile, the pile tolerates the greatest shear stress in its shell in comparison to the other piles. Which can be attributed to the excessive displacement of the pile. In the other words, the load- bearing capacity in the body decreases significantly. As can be observed, in this case the pile tends to buckle, and stress contours can be seen in a broader range at the tip of the pile.

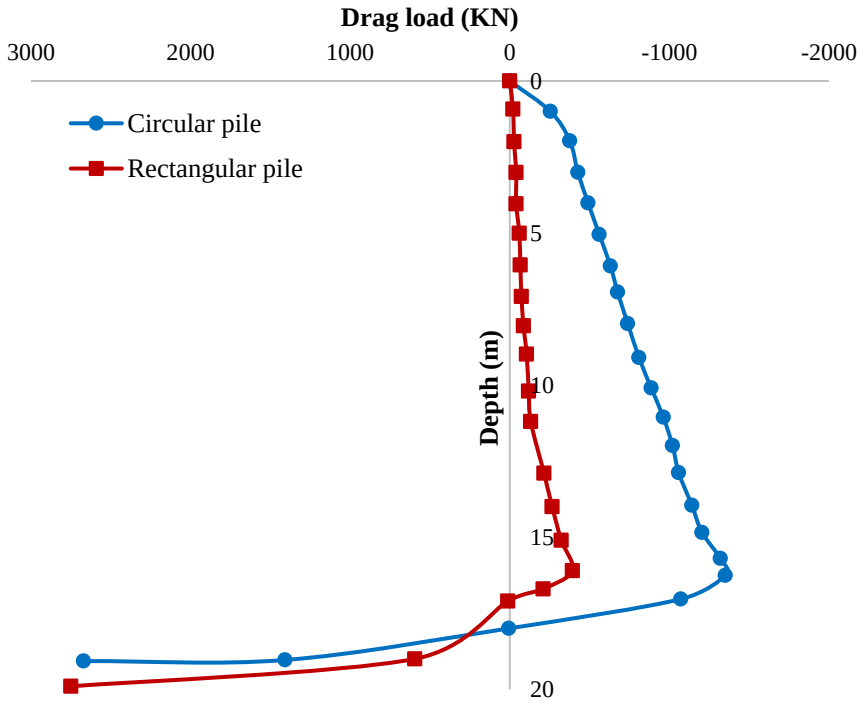

Fig. 15. Comparison of drag load in circular and square concrete pile

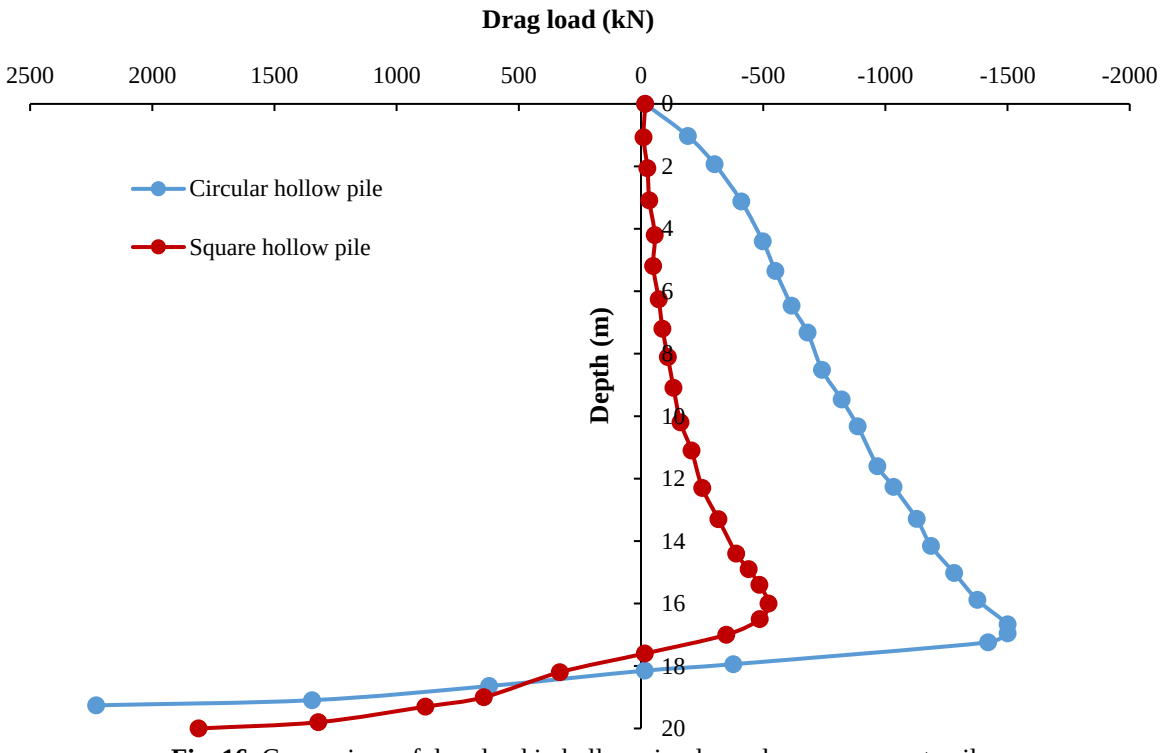

Fig. 16. Comparison of drag load in hollow circular and square concrete pile

It can also be stated that the negative friction occurs when the pile settlement is more than of the surrounding soil. In case of hollow piles, as well as other piles, the pile itself has a higher settlement than the surrounding soil. The hollow pile is expected to have more settlement than the soil surrounding, and negative frictional stress increase by negative frictional stress definitions. In the square pile, less negative frictional stress is observed due to its more surface area and higher density than the

surrounding soil. By making the hollow pile, the pile's density reduces which leads to an increase in the pile settlement. Finally, the pile is experienced with more significant negative frictional stress.

As shown in Figures 17 and 18, the soil stress bulb contours in case of circular and square pile types indicate that the concentration of stress in a circular state has occurred more than the squared shape at the tip of the pile and the stress bubbles in circular mode are wider than of the square. Thus, the soil needs more displacement to be failed and the bearing capacity and shear stress are increased on the pile body.

Table 2. Neutral plane location in different pile shapes

Neutral plane		
Pile type	**Pile settlement (m)**	**Neutral plane location**
Square composite (steel-concrete)	0.009	17.99
Circle composite (steel-concrete)	0.0095	17.82
Hollow circle	0.05	16.8
Hollow square	0.02	16.7
Simple square concrete	0.046	17.1
Simple circle concrete	0.04	16.99

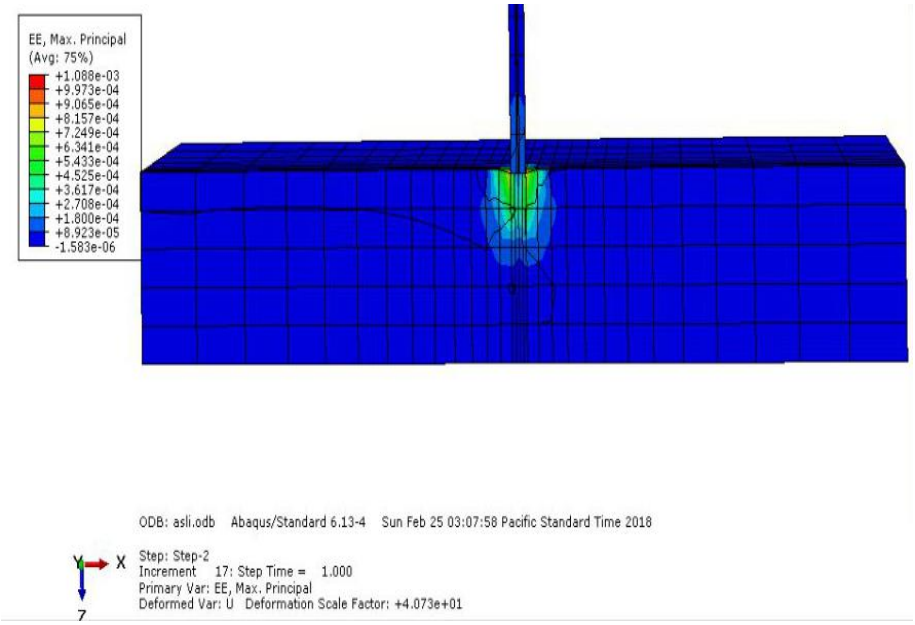

Fig. 17. The contour of stress bulb in the circular pile

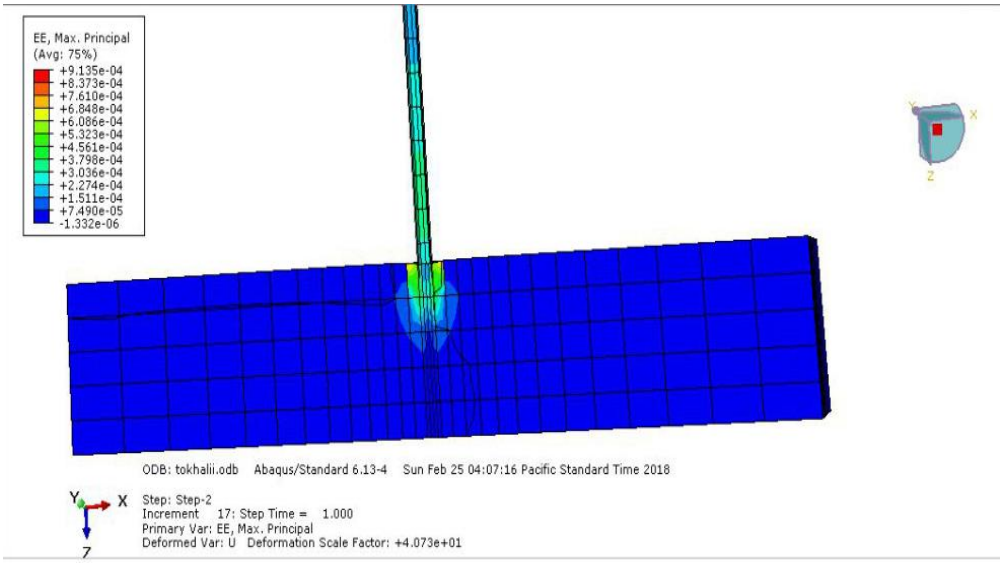

Fig. 18. The contour of stress bulb in the square pile

Table 3. Shear stress value in different pile types

Pile types	Maximum shear stress (kPa)
Simple square concrete	-9678.59
Square and circle composite (steel-concrete)	-933.003
Hollow circle	-48572.4
Simple circle concrete	-33929.6
Hollow square	-12776.5

9. Using the Uncertainty Method to Verify the Safety Reliability in NSF

In this paper, the uncertainty's effects of the input parameters on the negative skin friction of the pile were investigated. The impact of the uncertainty of input parameters on the pile design and negative skin friction phenomenon was studied by two methods of Finite Elements and an elasto-plastic model. Instability of the design parameters can reduce the load-bearing capacity of the soil and endangers the stability of the pile, which leads to uncertainty in the calculation.

Due to insufficient knowledge about the exact amount of design variables and its effect on reducing the load-bearing capacity, the uncertainty and probabilities can be used to assess a broader range in load-bearing capacity, settlement, and stress of the pile. After examining the Finite Element of the pile and the effect of negative skin friction on it, the estimation of negative frictional stress, soil-pile settlement, and drag load was investigated.

In this part, the use of uncertainty method and negative friction formulas, and soil settlement are discussed. In this regard, the induced stress and the pile settlement using numerical relationships were calculated. Afterward, taking input parameters randomly including the length, diameter, soil type load factors, and the safety level of the design's formulas were analysed. Besides the settlement rate, the negative skin frictional stress, and the load were calculated using the numerical relations. Further, the safety reliability was calculated by comparing the numerical values to the finite element model. In the end of the study, the relative distribution and accumulation curves of the pile's allowable load-bearing capacity, negative frictional stress, pile and soil settlements were plotted for fine-grained soils. Thus, appropriate statistical parameters (coefficient of variation, mean, etc.) have been extracted.

In this paper, by using a Monte Carlo simulation method, a probabilistic and straightforward relationship between definite reliability coefficient and the amount of stress variation due to negative skin friction and soil settlement has been established so that without using the comprehensive statistical information, the advantages of reliability analysis can be exploited.

In Figure 19, the settlement is obtained using Eqs. (1) to (5) for future steps.

$$\tau_0 = \sigma_0 \tan(\varphi_i - \theta) + \left(\frac{c_i sec\theta}{1 + tan\theta tan\varphi_i}\right) \quad (1)$$

$$\sigma_0 = K_0(q + \gamma z) \rightarrow (0 < z < H) \quad (2)$$

$$K_0 = (1 - sin\varphi)\gamma OCR^{0.5} \quad (3)$$

$$w_s = \xi\left(\frac{\tau_z r_0}{G}\right) \quad (4)$$

$$\zeta = ln\left(\frac{2.5L(1-\upsilon)}{r_0}\right) \quad (5)$$

By using the radial and vertical components of the interface stresses (σ_0 and τ_0), q: is the surface uniform loading; γ: is the total unit weight; K: is the coefficient of lateral earth pressure at rest; γ_{OCR}: is the over consolidation ratio and φ: is the soil's friction angle. r_0: is the pile's average radius, w_s: is the soil's vertical displacement, G: is the shear modulus of elastic soil, υ: is the Poisson ratio, and ξ: is the soil strain.

After calculating the settlement, the ultimate force input into the pile was calculated and calculated once again by applying the coefficient of this force and the

estimated safety reliability considering the limit function once for settlement and once for the final force. It comes with the least amount equal to the design index. Eq. (6) shows the base force F_b.

$$\frac{F_b}{(W_p)_b} = \frac{4r_b G}{(1-\upsilon)\eta_b} \quad (6)$$

where W_P: is the settlement of the piles, r_b: is the pile's radius, and η_b: is a coefficient considered for the depth of the pile base from below the surface chosen to be 0.88 in this work. The value of this force is shown in Figure 22 as F_b that once obtained with a coefficient of 1.3 and one without coefficients.

After placing in the Eq. (1), the safety reliability is calculated, once with the criteria of the settlement is obtained, the minimum number is depicted as the safety reliability in Figure 23 which is available u_p to this stage in this research.

$$Q_{(Ult)} = C.N_c + Q.N_q + 0.5.\ \gamma.\ B.\ N_\gamma \quad (7)$$

But then, with the estimated final load, the amount of pile's bearing capacity was calculated and eventually reported the safety reliability. In other words, using Eq. (7) for bearing capacity, the amount of design load can be estimated while the statistical information and its coefficients for the circular and squared shape piles are not available.

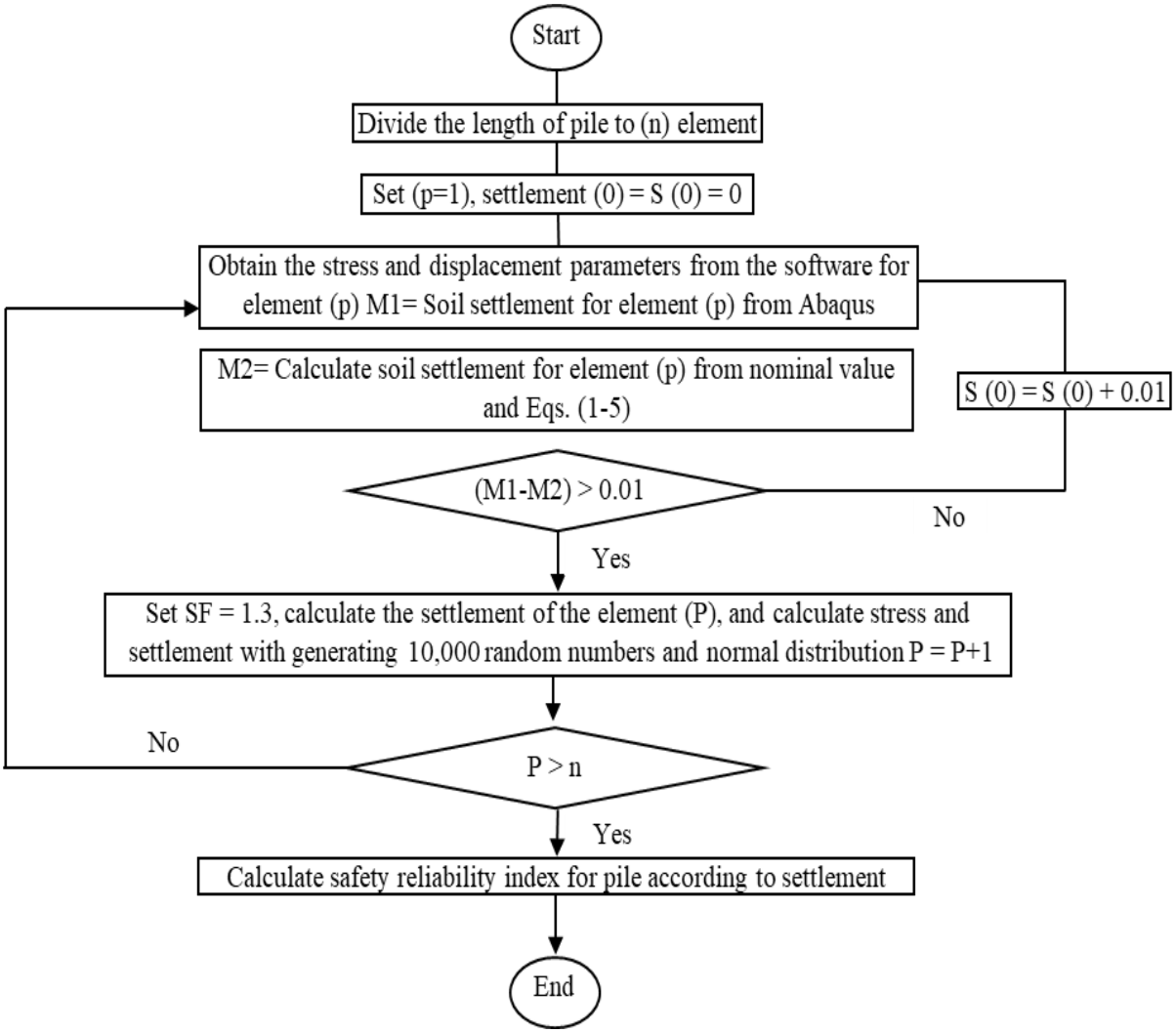

Fig. 19. Flowchart based on Monte Carlo method in NSF in MATLAB software

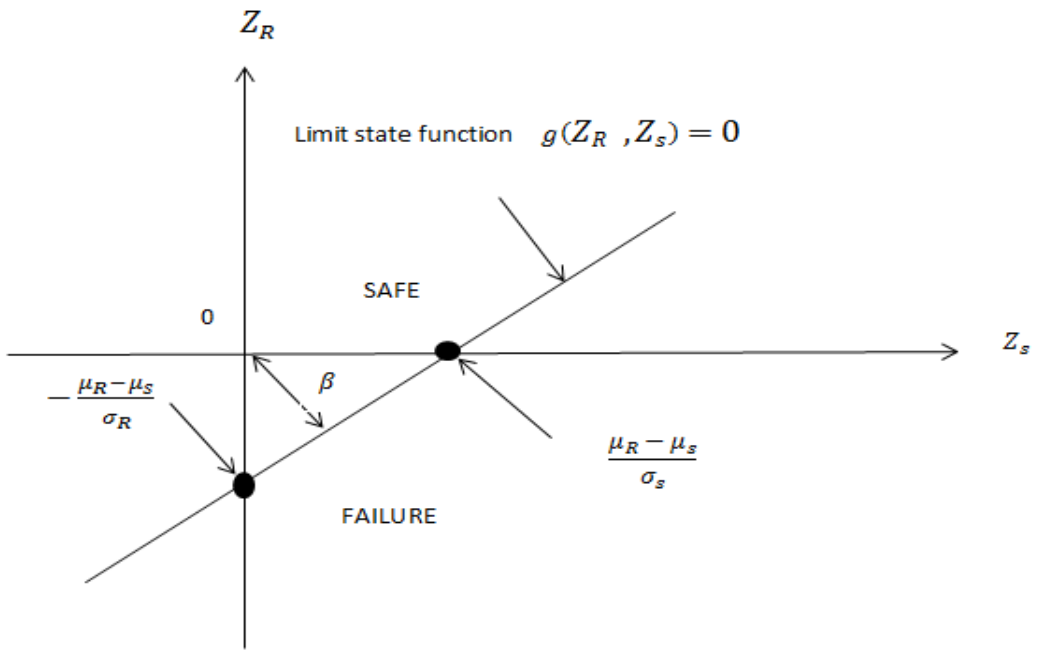

Fig. 20. Reliability parameter index as the shortest distance from the reduced variables to the origin Melchers et al. (2018)

10. Determining the Uncertainly for Each Design Parameter

In order to generate random design parameters, it is necessary to consider the mean, variance, and statistical distributions for generating random numbers in MATLAB user guide (1998). In this section, the design parameters and their statistical values are presented. Design parameters values, statistical distribution considered and variance of model design parameters are shown in Table 4. The vertical coefficient of loading in the design equations is 1.3, and soil settlement is calculated considering the random parameters of the pile and soil as well as the corresponding coefficient.

11. Safety Reliability

The limit function of the design in the present problem is *g(x) = R-L*, in which *L*: is the actual settlement value obtained from the pile in the ABAQUS software, and *R*: is the design function that is the amount of calculated settlement with design formulas. According to Figure 20, safety reliability is defined as the shortest distance from the origin of the reduced variables to limit function line g(x). The safety reliability is calculated as the shortest distance from the source of the Eq. (8) (Comodromos et al., 2005).

$$\beta = \frac{\mu_R - \mu_L}{\sqrt{\sigma_R^2 + \sigma_l^2}} \tag{8}$$

where β: is the inverse of the coefficients in the formula *g(R,L) = R-L*, when *R*, *L* are not interdependent. There are no correlation relations between *L* and *R*.

The safety reliability β is dependent on the failure surface by Eq. (9).

$$\beta = -\phi^{-1}(pf) \tag{9}$$

The following steps are taken to estimate the safety reliability:

• Generate 10,000 random numbers for the variables presented in Table 4 using variances, probability functions, and mean parameters

• Using design formulas by entering the vertical load factor to calculate the soil settlement

• Estimating the safety reliability value using Eq. (2).

Table 4. A stochastic model for concrete piling in cohesionless soils (Kok-Kwang Phoon et al., 2015; Lee, 2001)

Parameters	Probability density function	Mean values	Coefficients of variations
Pile dimension (D)	Normal	0.4	0.03×D
Soil density (y)	Normal	18000	0.15
Cohesion (C)	Normal	30000	0.15
L	Normal	20	0.03×D
$\emptyset$	Normal	20	0.15
Stress (σ_n)	Normal	Vertical stress from each element	1.1× σ_n
Shear module	Normal	$\frac{E}{2 \times (1+\vartheta)}$	-

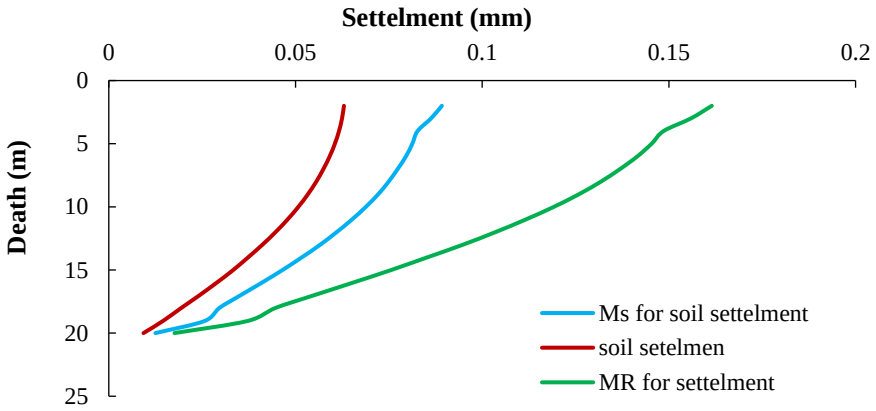

Fig. 21. The calculated settlement rate by generating random numbers with a vertical stress coefficient of 1.3 and without vertical stress coefficients

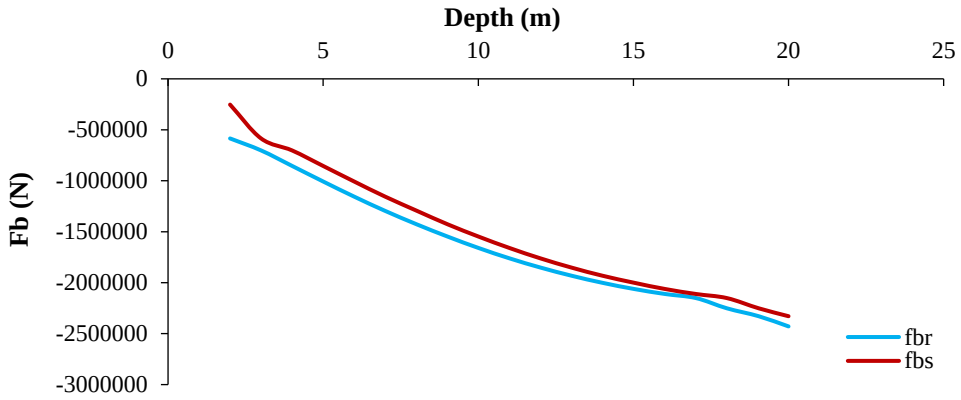

Fig. 22. The rate of calculated Fb by generating random numbers with a vertical stress coefficient of 1.3 (MFb_R) and without vertical stress coefficients (MFb_s)

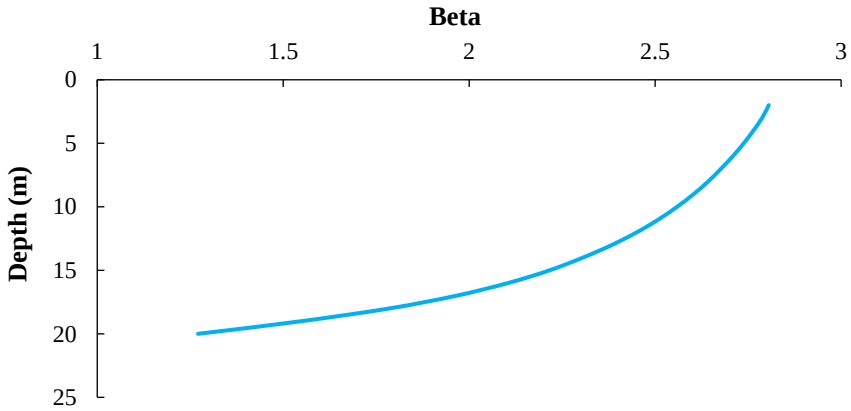

Fig. 23. Safety indicator for design formulas

According to Figures 21 and 22, in the settlement design methods considered for the pile, the number 1.3 as a reliability coefficient and load coefficients (1.5 for dead load) is greater than the values calculated by the software. This is the main reason for the design coefficients in numerical formulas. The highest settlement of soil and piles is observed at the top of the pile. The imported coefficients have a greater effect on numerical methods. This difference is reduced by increasing the depth of the pile and decreasing the settlement. Decreasing the dead load coefficients entered in the design as well as the safety factor decrease this difference. This was because these coefficients were not entered in ABAQUS software and the calculated values for the settlement were obtained according to the actual amount of the load. In contrast, in the calculated numerical values, constant coefficients were used. The difference in numerical values calculated by the design formulas and the Finite Element values are available in other studies such as Badarloo and Jafari (2019) and Akbari and Jafari (2018). The existence of these differences led to a safe design. Because the safety surface obtained by proposed design formulas was always greater than software values and pile will have excellent stability.

Figure 21 shows the rate of soil settlement, taking into account the production of random design parameters. The Mr represents the calculated settlement regarding coefficient 1.3 for the vertical stress. MS represents the estimated settlement without the design coefficient. Figure 22 shows this value for the pile's end force, obtained by producing designing coefficients and random numbers and proposed formulas in regulation. The amount of safety reliability for a pile is given by Eq. (2) and is shown in Figure 23. The results show that with increasing depth, the safety reliability increases; however, the calculated number depends on the variance and probability distributions that are correctly entered into the Monte Carlo cycle, and the changing the parameters leads to a change in response to the safety reliability.

12. Factor of Safety

Using the pile testing and site investigation level, Table 5 indicates the recommended minimum factors of safety that should be implemented in the design of piles. Besides, values should be adjusted to allow for extraordinary factors on a particular development. According to Table 5, the design coefficient for the desired piles is higher than 2.5, which reflects the fact that the use of the coefficient of 1.3 for vertical stress can provide reliable results in design.

13. Conclusions

The purpose of this study was to investigate the negative skin friction on composite piles' design. One of the innovations obtained in the present study was using the reliability method to design a pile under negative skin friction and comparing the values with software results. To do this, the rate of the pile's settlement was estimated by using a random number generation. Using the Monte Carlo reliability method, the influence of model input parameters on calculated settlement results with software modelling was compared with existing theoretical relationships. Another innovation of the present study was to examine the composite types, filled and hollow piles with the areas of different sections and their effect on soil settlement under the influence of negative skin friction. The results showed that the elastic modulus and the weight of the pile have a significant impact on the pile settlement.

The following conclusions can be drawn from this study.

Table 5. Minimum factors of safety for piles (Local Authority Building Control Technical Information, 2010; Kong Gang-qiang et al. 2014)

Testing level	Level of site investigation		
	Full	**Limited**	**Minimum**
Full	2	2.25	2.5
Limited	2.25	2.5	3
None	2.5	3	3

- In order to study the impacts of negative skin friction on composite piles, it is necessary to consider the pile mass concerning different modes. In other words, according to the relation $F\text{-}F_k = m.\delta$, friction depends on the mass and the stiffness of the pile. Based on the definition of the friction theory, the ratio of the pile settlement and the force applied to the pile is different from that of the filled pile. $F\text{-}F_k = m.\delta$, $Fk = \mu.mg$, as the friction force decreases in the body of the pile, the displacement (due to the second-order differential of the acceleration) is applied to the structure. In other words, in the hollow sections, by reducing the mass of the pile, less force and less frictional stress in the pile's shell is generated.
- Using a steel pod in a composite pile, the amount of soil settlement around the composite pill is lower than the soil settlement around the filled concrete pile. The settlement of the composite pile is also smaller than filled concrete piles. The settlement of filled circular concrete piles (square and circle) is lower than the filled square concrete pile. The amount of settlement in hollow piles is more than the other ones.
- In the circular sections, the value of the drag load is more than of the square-shaped sections in both composite and hollow sections. Besides, in the hollow sections, the amount of drag load in the circular concrete sections is greater than the square sections.
- In composite piles, the amount of negative shear stress is more than all the discussed models in the numerical study. On the other hand, the more stress at the tip of the pile occurs; the greater amount of drag load is tolerated. In other words, a neutral plane occurs in greater depth along the pile length. In case of the square composite pile, the neutral plane is more in-depth than all of the models.
- MS values, which are non-coefficient values, show lower settlement at the same depth than of the load with a coefficient (Mr), and both of these settlements are higher than of the calculated theory. Also, the reliability index computed using the Monte Carlo method decreases with increasing the depth of the pile. One of the reasons can be more uncertainty in determining the input parameters obtained in the pile settlement calculations. In other words, the higher the accuracy of the input parameters and the reliability index, the lower the final safety factor coefficient will be.
- Ultimately, drag load, soil and pile settlements and factor of safety coefficient have been obtained for verification. Thus, drag load has been generated by cumulative forces that mobilized around the pile's shaft by surcharge and the numerical point defined on the pile's length. After running the software, these force's points have been read and interpreted.

14. References

Akbari, J. and Jafari, F. (2018). "Calibration of Load and Resistance Factors for Reinforced Concrete", *Civil Engineering Infrastructures Journal*, 51(1), 217-227.

Azizkandi, A., Taherkhani, R. and Taji, A. (2019). "Experimental study of a square foundation with connected and non-connected piled raft foundation under eccentrically loaded", *Civil Engineering Infrastructures Journal*, 52(1), 185-203.

Badarloo, B. and Jafari, F. (2019). "Numerical study on the effect of concrete grade on the CFT circular column's behavior under axial load", *Civil Engineering Journal*, 5(11), 2359-2376.

Cao, W., Chen, Y. and Wolfe, W.E. (2014). "New load transfer hyperbolic model for pile-soil

interface and negative skin friction on single piles embedded in soft soils", *International Journal of Geomechanics*, 14(1), 92-100.

Carswell, W., Arwade, S.R., DeGroot, D.J. and Lackner, M.A. (2015). "Soil-structure reliability of shore wind turbine monopile foundations", *Wind Energy Journal*, 18(3), 483-498.

Comodromos, E.M. and Bareka, S.V. (2005). "Evaluation of negative skin friction effects in pile foundations using 3D nonlinear analysis", *Computers and Geotechnics*, 32(3), 210-221.

Ditlevsen, O. and Madsen, H.O. (2007). *Structural reliability method*, Wiley, New York.

El-Mossallamy, Y.M., Hefny, A.M., Demerdash, M.A. and Morsy, M.S. (2013). "Numerical analysis of negative skin friction on piles in soft clay", *Housing and Building National Research Center HBRC Journal*, 9(1), 68-76.

Eslami, A., Lotfi, S., Infante, J.A., Moshfeghi, S. and Eslami, M.M. (2020). "Pile shaft capacity from cone penetration test records considering scale effects", *International Journal of Geomechanics*, 20(7), 04020073.

Fardis, M.N. and Veneziano, D. (1982). "Probabilistic analysis of deposit liquefaction", *Journal of Geotechnical and Geoenvironmental Engineering*, 108(3), 395-417.

Gang-qiang, Z.K., Han-long, L., Xuan-ming, D. and Liang. R. (2014). "A simplified approach for negative skin friction calculation of special-shaped pile considering pile-soil interaction under surcharge", *Journal of Central South University*, 21(9), 3648-3655.

Golafzani, S.H., Chenari, R.J. and Eslami, A. (2019). "Reliability based assessment of axial pile bearing capacity: static analysis, SPT and CPT-based methods", *Journal of Georisk: Assessment and Management of Risk for Engineered Systems and Geohazards*, 1-15.

Haghbin, M. and Ghazavi, M. (2016). "Seismic bearing capacity of strip footings on pile-stabilized slopes", *Civil Engineering Infrastructures Journal*, 49(1), 111-126.

Hajitaheriha. M.M. and Hassanlourad. M. (2015). "Numerical modeling of the negative skin friction on single vertical and batter pile", *Acta Geotechnica Slovenica*, 12(2), 47-55.

Huang, T., Zheng, J. and Gong, W. (2015). "The group effect on negative skin friction on piles", *Procedia Engineering*, 116, 802-808.

Jaky, J. (1948). "Pressure in silos", Proceedings of the *2nd International Conference on Soil Mechanics and Foundation Engineering*, Rotterdam, Netherland, 1, 103-107.

Jha, S. K. and Kiichi, S. (2009). "Reliability analysis of soil liquefaction based on standard penetration test", *Computers and Geotechnics*, 36(4), 589-596.

Jinyuan, L., Hongmei, G. and Hanlong, L. (2012). "Finite Element analyses of negative skin friction on a single pile", *Acta Geotechnica*, 7(3), 239-252.

Juang, C.H., Jianye, C. and Zhe, L. (2012). "Assessing SPT-based probabilistic models for liquefaction potential evaluation: A 10-year update", *Journal of Georisk: Assessment and Management of Risk for Engineered Systems and Geohazards*, 7(3), 137-150.

Lee, C.J. (2001). "The influence of negative skin friction on piles and in pile groups", Ph.D. Thesis, Cambridge University.

Lee, C.J., Bolton, M.D. and Al-Tabbaa. A. (2002). "Numerical modeling of group effects on the distribution of drag loads in pile foundations", *Geotechnique*, 52 (5), 325-335.

Local Authority Building Control Technical Information Note 3. (2010). *Driven and in-situ piled foundations*, Cambridge City Council, East Cambridgeshire District Council, Fenland District Council, Huntingdonshire District Council, Peterborough City Council, South Cambridgeshire District Council, 1.

The MathWorks, Inc. (1998). *Matlab user guide*, Natick, MA.

Melchers, R.E. and Beck. A.T. (2018). *Structural reliability analysis and prediction*, John Wiley & Sons.

Moshfeghi, S. and Eslami, A. (2018). "Reliability-based assessment of drilled displacement piles bearing capacity using CPT records", *Marine Georesources and Geotechnology Journal*, 37(1), 67-80.

Pastor, J.L., Marcos, O.J., Miguel, A. and Climent, I.S. (2018). "Skin friction coefficient change on cement grouts for micropiles due to sulfate attack", *Construction and Building Materials*, 163, 80-86.

Phoon, K.K., and Ching, J. (Eds.). (2018). *Risk and reliability in geotechnical engineering*, CRC Press.

Xing, H. and Liu, L. (2018). "Field tests on influencing factors of negative skin friction for pile foundations in collapsible loess regions", *International Journal of Civil Engineering*, 16(10), 1413-1422.